# A MECHANISM TO EXPLAIN PARTICLE SIZE SEGREGATION AND BINDER DEPLETION DURING COATING

Richard E. Gagnon
Protein Technologies Int'l
1034 Danforth Avenue
St. Louis, MO 63102

Thomas D. Parish
Potlatch Corporation Fiber Research Center
20 North 22nd Street
Cloquet, MN 55720

Douglas W. Bousfield
Paper Surface Science Program
Department of Chemical Engineering
University of Maine
Orono, ME 04469-5737

## ABSTRACT

Observations of coating processes frequently reveal increasing coating solids, decreasing binder content and increasing average pigment particle size in the recycle loop. Product quality can decrease due to these changes in coating composition. Observations made during production-scale experiments are presented. The experiments demonstrated time-dependant variations in paper properties and coating composition.

A new mechanism is proposed to explain the time dependent size segregation of pigment particles, as well as the depletion of binder and other organic species. Forces experienced by the coating during application, and consolidation prior to metering result in acceleration perpendicular to the web of all coating components. A differential acceleration of pigment particles and colloidal material results from differences in particle diameter, density, and the effects of viscous drag. This differential acceleration produces a non-uniform z-directional displacement of components and non-homogeneity in the wet coating film. The wet coating layer metered and returned to the machine supply is different from both the bulk supply and the coating which has actually been applied to the sheet. For reasonable values of dewatering, viscosity, and particle size, the equations predict a separation of large and fine particles. The theoretical predictions are compared to production scale data.

## INTRODUCTION

The unique functional properties of paper coatings are derived through both process and formulation. Predictable performance for the end user is critical, and depends on consistent composition of both the basesheet and coating layer. In production, quality coordinators reject or release paper based on the results of standard tests measuring essential properties.

In certain applications, paper properties are far from constant. Variations in sheet gloss, pick strength, and fiber coverage are time dependent; with acceptable properties achieved early in a run and declining as the run continues. Reductions in gloss potential can result in decreased productivity through finishing processes. Poor fiber coverage, and pick strength can translate into complaints from printers. In-house losses due to substandard quality detract considerably from the profitability of the machine. Certain compositional changes over time will produce the results noted; decreasing binder content and an increase in the pigment size distribution will exhibit just these kinds of changes.

An equilibrium state in sheet and coating properties can be reached during the run, controlled by mass balance. This equilibrium condition is lost when fresh coating is no longer supplied to the machine or during periods of high dilution (during start up or a run-out prior to grade change). These periods result in compositional changes that are both large in magnitude and rapid in rate. Industrial experience indicates that binder loss and size segregation are aggravated by the following process conditions:

1) Application solids well below the first critical concentration (FCC)
2) Large pressure pulses / high rates of dewatering from application to metering
3) High re-circulation rates
4) Large volumes of supply coatings

Although the term "coating fractionation" is familiar to many individuals, a definition is in order. The processes we are describing occur when excess coating is applied to the web, the excess is metered, and this metered material is returned to the machine supply. Production data demonstrate that over time, coating solids increase, the total quantity of binder in the coating decreases, and the particle size distribution (PSD) becomes coarser.

The exact nature of the process of fractionation and the factors that influence its rate and magnitude are poorly understood. Little if any reference exists in the literature to studies describing the phenomenon directly. Lennartz et al. (1987) and Wineland et al. (1989) describe helix flows to separate large and small particles. Work presented in the late 1980's (Eklund and Salminen 1986) and further developed during the 1990's (Eklund and Letzelter 1993; Salminen *et.al.* 1995; Lohmander *et.al.*1999*)* provide points of departure for this discussion. Essentially focusing on pressure dewatering and consequent filter cake formation, these models predict an increase in solids content in the coating layer at the substrate / coating interface. However, these models have not been extended to predict the time-dependant changes in composition that have been observed. Filtration alone of suspensions can generate gradients in particle size from top to bottom of a filtercake, with fine material being transported deeper into the filtercake. This phenomena may explain some of the results seen during coating trials. Sedimentation of particles also can generate size segregation of particles. During a coating operation, sedimentation is too slow to be of importance. Here we propose a new mechanism that may explain the size segregation of materials during coating.

## EXPERIMENTAL OBSERVATIONS

In the following two cases, data and observations from production scale experiments are reported.

### *Case 1) On-machine Gloss Grade*

The Billblade™ is a puddle coater with blade metering on one side of the sheet and a forward roll on the other (both sides of the sheet are coated simultaneously). Coat weight in this application depends on application solids, and on water retention. Film split patterning (orange peel) and side-to-side differences in coat weight have been shown to depend on coating rheology.

During the course of a production trial of a supercalendered grade, the following observations were made regarding coating properties, sheet quality and finishing parameters:

- Coat weight distribution became increasingly two-sided, as indicated by ammonium chloride burnouts of each reel produced. The burnouts also indicated declining fiber coverage at equal coatweight applied.

- Although coating solids were held relatively constant, the Brookfield viscosity of the coating decreased, and water retention values (as measured with the AA-GWR) increased.

- At the supercalender, decreased line speed, along with increased nip load and stack temperature was required to reach target gloss as the run progressed. Despite the use of steam, the gloss of the sheet became increasingly two-sided.

Coating samples taken during the trial were evaluated to determine; clay / carbonate ratio, pigment particle size distribution, and total organic content. The results of those evaluations showed that the level of calcium carbonate (relative to kaolin) in the formula was increasing over time, and that the total level of organic material in the coating was declining.

**Table 1**. Provides a summary of pigment particle size distribution (PSD) data as a function of time during this trial. The coating sample associated with t = 0 minutes is a sample of the coating as it was recirculating on the paper machine at the outset of the trial. The second sample was taken after 30 minutes were elapsed. The data shows significant changes had taken place in the pigment PSD.

**Production coating samples**

| | **Mass Percent finer than specified Equivalent Spherical Diameter** | | | | | |
|---|---|---|---|---|---|---|
| | **5 µm** | **3 µm** | **2 µm** | **1.5 µm** | **1 µm** | **Avg** |
| t = 0 min | 97 | 89 | 85 | 82 | 62 | 0.9 µm |
| t = 30 min | 94 | 78 | 73 | 68 | 53 | 0.98 µm |

***Table 1. Particle size distribution vs. time.***

Coating samples were prepared as follows for particle size distribution analysis. Samples were diluted to 6% solids with a 0.01% tetra-sodium pyro-phosphate solution. Samples were ultra-sonicated for 5 minutes, the sample temperature reaching approximately 60° C, and being returned to 31° C in a water bath with constant stirring prior to introduction to the instrument. The starting diameter for the analysis was 50 microns, and the scan rate was set to 472 (scan rate

is a function of the density of the materials evaluated as well as the viscosity of the suspending medium). These operating parameters were established in previous studies conducted to determine the suitability of this technique for the purposes of evaluating whole coatings, as opposed to single pigment samples.

These coating samples were subsequently applied to woodfree basepaper, and supercalendered. **Table 2** shows the important implications of the phenomena. The coating sampled after 30 minutes of operation produced lower initial gloss, 2 nip, and 4-nip gloss than the values obtained with the coating sampled at start-up. The gloss potential of the coating declined, and there is some uncertainty as to whether the target gloss could be reached even with modified supercalander operating parameters (reduced line speed, higher nip loads, increased temperature, and use of steam). In production, this phenomenon can lead to rejected production. Other details of the production run are given later in the paper.

**Production coating samples applied to basestock**
**Laboratory supercalendering conditions were 32° C, 140 KN/m**

| | 0 nips | 2 nips | 4 nips |
|---|---|---|---|
| t = 0 min | 23 | 58 | 64 |
| t = 30 min | 14 | 46 | 53 |

***Table 2. Gloss potential vs. time.***

The critical issue is that during the trial, dilution water was required to keep coating solids constant (as noted above). This observation is common for many coating operations. Some mechanism is operating which separates pigments from the aqueous phase. This mechanism is operating on a level that evaporation cannot explain. The other important observation is in table 1; the average pigment size increases over time. This data shows that somehow, fine pigment particles are being separated from large pigments and are removed from the system during application and metering.

### *Case 2) Basestock Surface Treatment*

In a second case, an experimental surface treatment was applied on the paper machine, to a woodfree publication grade basepaper. This paper was subsequently top coated off machine. Coating application solids were held relatively constant through automatic dilution, which averaged 0.45 gallon/minute. Coating samples were taken from the machine supply tank. The coating was 55 and 45 parts $CaCO_3$ and Kaolin, respectively, with 21 parts total binder. The rheologic properties and composition (organic content, clay: $CaCO_3$ ratio, and Particle Size Distribution) of these samples were characterized as functions of time. **Table 3** provides a summary of coating rheology and composition as a function of time. Notice that the carbonate is the large pigment in this case.

| Time (Minutes) | % Solids | BV 20 rpm (#2 spindle) | Differential Ash and Leco $N_2$ Analysis | | | |
|---|---|---|---|---|---|---|
| | | | Parts Kaolin | Parts $CaCO_3$ | Parts Organic | Parts $N_2$ binder |
| 0 | 56.8 | 1700 | 45 | 55 | 21 | 6.0 |
| 80 | 58.5 | 1000 | 41 | 59 | 17 | 4.8 |
| 450 | 58.9 | 850 | 41 | 59 | 12 | 4.6 |
| 575 | 59.5 | 950 | 41 | 59 | 11 | 4.6 |

***Table 3. Coating viscosity, and parts analysis vs. time.***

The data shows significant changes in the viscosity and composition of the coating as a function of time. In **Figure 1,** data generated through both differential ash and nitrogen analysis are presented. This figure shows a significant decrease in the total organic content as well as loss of nitrogen containing materials. We have interpreted these results as an indication of a loss of latex and soluble polymer from the coating during the run. The level of polymer decreased by approximately 25%, as opposed to a reduction of approximately 48% in total organic content. This is likely the result of a higher degree of association between the soy polymer and pigment than that between the lattices and pigments. The pigment particle size distributions of the coating samples were conducted as described above and are shown in **Figure 2**.

As seen in the data from Case 1, the pigment particle size distribution changes dramatically from its original values. The change was greatest during the early portion of the trial, and while the data does not indicate a true equilibrium state, the rate of change slows significantly.

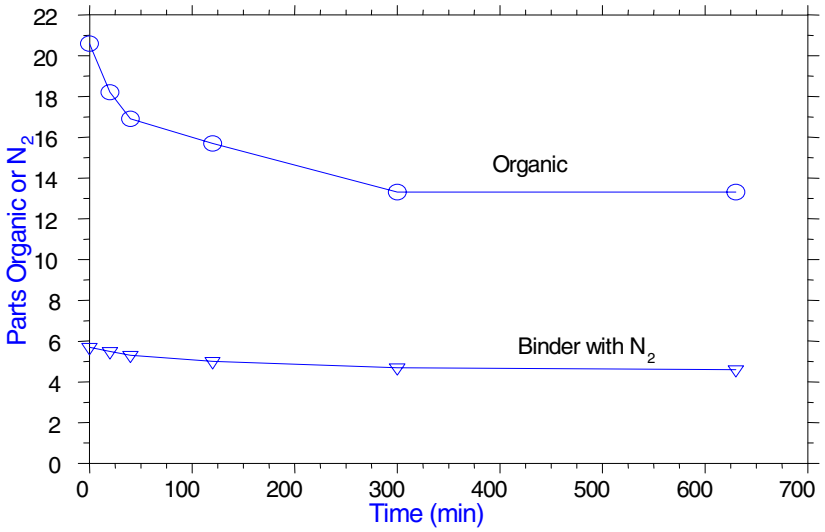


***Figure 1. Differential ash analysis / Leco $N_2$ results of production run showing the depletion of binder during a run.***

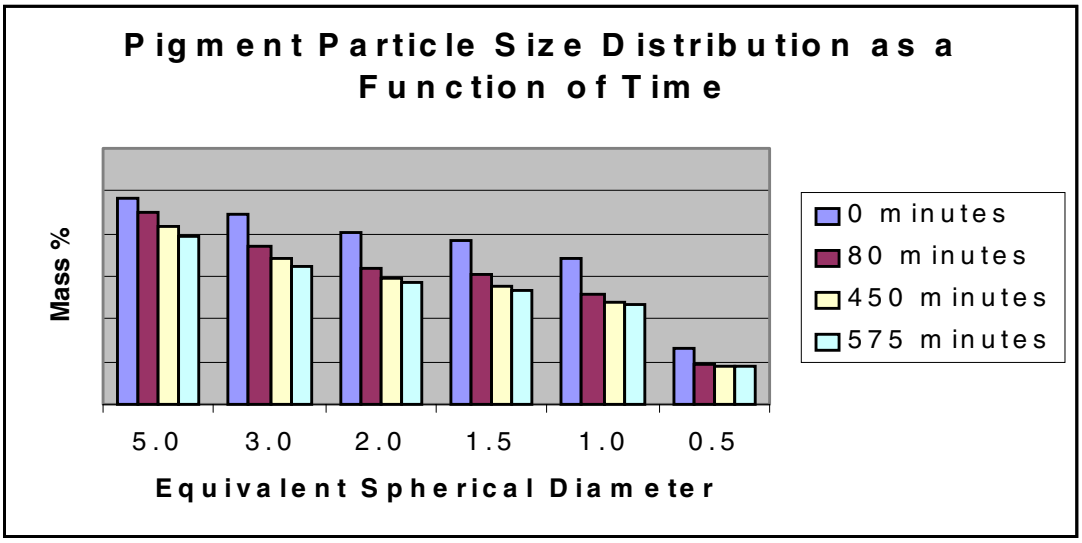


*Figure 2. Particle size distribution changes during production run. Results show an increase in the average particle size.*

One of the objectives of the trial was to improve the final stiffness of the coated, finished sheet. **Figure 3**, below provides a summary of supercalendering conditions and the net gain in final stiffness of the trial versus a control reel manufactured early in the following grade run. Supercalendering conditions were constant throughout this trial, with temperature at 50 C and 350 KN/m. The data clearly indicates declining gloss potential and sheet stiffness.

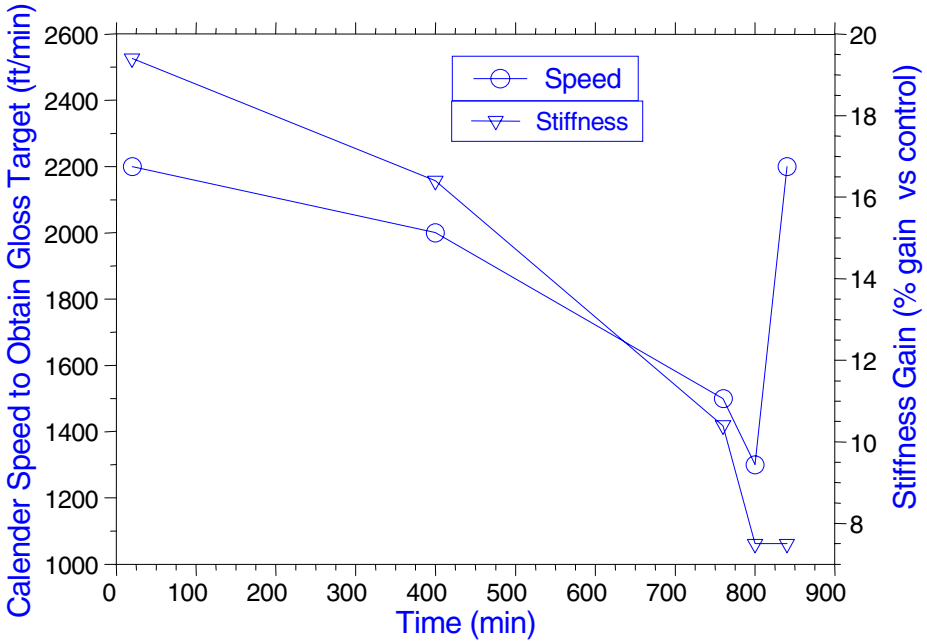


*Figure 3. Calender speed required to reach target gloss and stiffness gain during a production run.*

The reel produced at 840 minutes was the final reel of the basestock run in Figure 3. At this point in the process, all available coating had been pushed to the paper machine in preparation for a grade change. In an attempt to establish the relative impact of supercalendering conditions on final sheet stiffness, this reel was top-coated with a formula significantly greater in gloss potential than the control topcoat.

While the supercalendering conditions for this final basestock reel were identical to the first, the data did not indicate any improvement in sheet stiffness. The conclusion drawn at the time was that in this case, final sheet stiffness was highly dependent on the properties of the basestock, and that basestock stiffness was highly dependent on precoat composition and holdout.

The data presented above paints a picture of a coating that changed dramatically with time, resulting in lost productivity and a sheet with properties very different from those intended by the experimenters. In the following sections, we provide a review of past theories, present a new and unique mechanism to explain the phenomenon we have described, and compare values calculated from our model to those experimentally obtained.

## THEORETICAL

### *Mechanism*

In most coating application systems coating suspension is applied in excess of that needed to reach a target coat weight. The excess is metered and returned to the machine supply system. When there is penetration of liquid phase into the web, there is a velocity component perpendicular to the web. This penetration velocity is a complex function of the web porosity, the coating formulation, and the process conditions. There have been a few attempts to calculate the penetration velocity in blade coating of paper. Chen and Scriven (1988), using the pressure pulse calculated from a finite element method, predicted the amount of penetration into the web in the applicator roll and under the blade. They took into account a number of factors, including the compression of trapped air in the web. Letzelter and Eklund (1993) calculated the dewatering and the growth of the filtercake making certain assumptions about the pressure field under the blade. Bousfield (1995) calculated simultaneously; the pressure distribution, filtercake formation, and the amount of penetration in a hypothetical blade coating operation. Operational limitation predictions compared well with pilot scale data.

**Figure 4** is a schematic of the production operation with coating on both sides. We have sketched also a hypothetical filtercake layer on both sides of the web. The coating is supplied in excess to both sides of the web. The roll-web nip meters the coating on one side and the blade-web nip meters the amount of coating on the other side. The metering action is near the exit of the blade. Excess coating is removed from the nips in a regular manner. The same basic action should occur for bent, stiff or other blade metering systems. For illustrative purposes, we will focus our attention to the blade side of the coater in the next few figures.

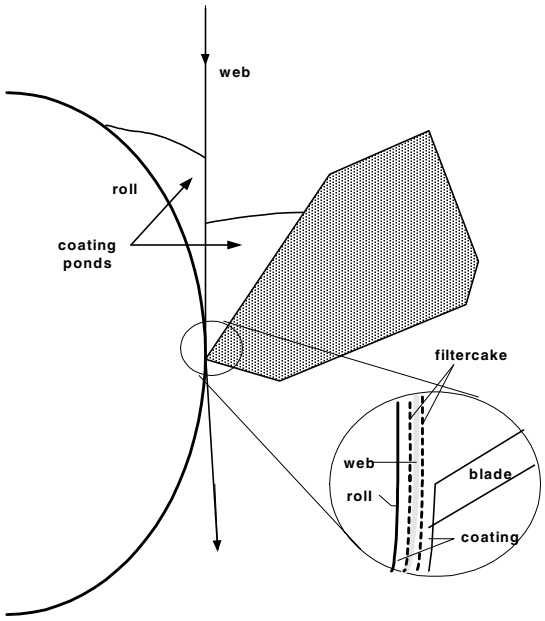


***Figure 4. Schematic of the production coater with blowup of nip region.***

Although increasing solids and a buildup of coarse materials during coating operations have been observed for a number of years, a good mechanism has not been proposed to describe these processes. A simple filtercake model does not explain the results, because any filtercake that is formed on the web also passes under the metering element. The net result is that the coating returned to the supply is essentially equivalent to that which was applied. This situation is depicted in **Figure 5**.

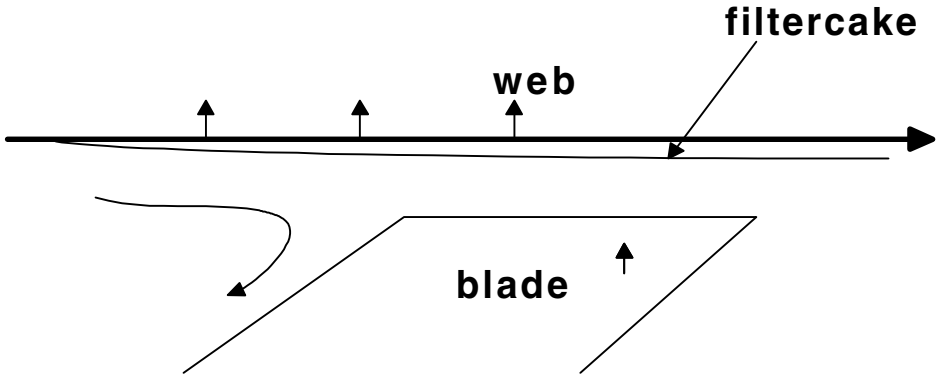


***Figure 5. A schematic of filtercake formation during coating. The coating returned to the machine supply is at the same solids as the original coating. Blade-web gap is larger than reality for illustrative purposes.***

The schematic in Figure 5 does not show the actual situation in terms of the roughness of the base paper. Actually, the paper is rough compared to the average gap between the blade and the paper. In addition, non-uniformity of the web might induce localized rapid drainage and filtercake formation. Metering of excess coating from these areas of non-uniformity could result in an overall increase in the solids of the coating being returned to the machine supply. This mechanism would explain the increase in solids, but it would not explain why the pigment

systems become coarser. Therefore, it is possible that regions of filtercake are actually scraped off by the blade increasing the solids in the recycle line. If fine particles are separated due to filtration and move towards the web or even into the web, an argument could me made that this mechanism would also increase the particle size distribution. However, this has not been discussed or studied in the literature and it is questionable that the blades can scrape off filtercake without degrading product quality.

Another possible mechanism to describe the behavior of the applied coating film is a "thickening" of the coating that occurs due to dewatering; the returning coating is at higher solids. Here, a solids gradient is formed due to dewatering. The coating along the blade surface is still at the original solids, but coating solids increase with increasing proximity to the coating basestock interface. This is similar to the recent calculations of Brotz et al. (1997) that predict gradients in solid under the blade. However, these calculations show that the returned solids are essentially the same solids as the original. **Figure 6**, may be taken to represent the results of Brotz et al. (1997), showing that all of the coating layers having increased solids also pass under the blade.

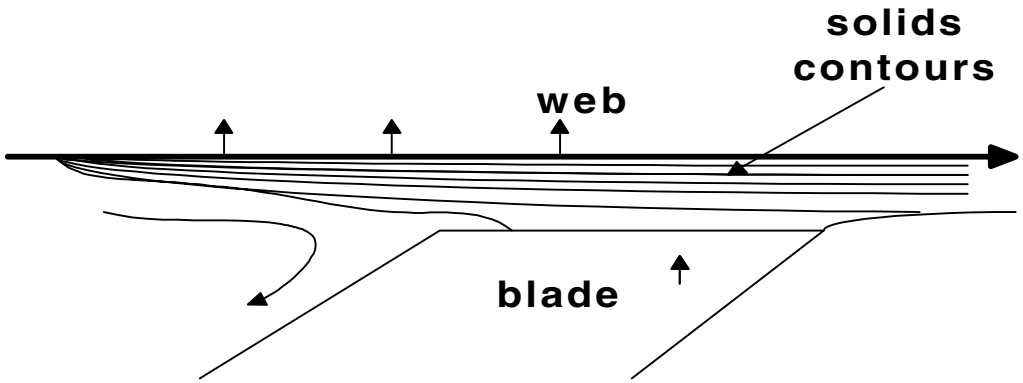


***Figure 6. A representation of the results of Brotz et al. The coating layer metered by the blade is very nearly at the original solids.***

The results of Toivakka and Eklund (1997) suggest a mechanism that would result in larger particles being selectively metered away from the web and small particle being caught with the web. This mechanism is illustrated in **Figure 7**: large particles are pushed away from the web by the smaller pigment particles. Intuitively, however, this mechanism would seem to act over a small layer, does not explain the increase in solids, and does not explain the results with porous webs.

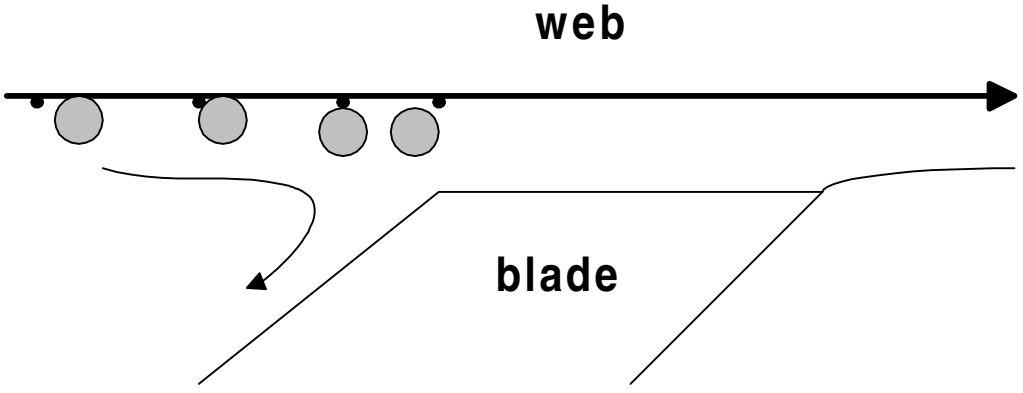


***Figure 7. A representation of results expected based on the work of Toivakka and Eklund. Fine particles close to the web are able to push larger particles away from the web.***

Our proposed mechanism is described in **Figure 8**. Here, large particles are separated from the liquid phase and from small particles, near the stagnation streamline, due to pulse dewatering. The greater inertia of large particles, relative to that of fine particles, is the key factor in this separation. Because the fines and the liquid phase move relative to the larger particles, there is a separation near the stagnation streamline. The degree of filtercake formation does not influence this mechanism, other than providing a limit to the magnitude (rate) of dewatering. Note that if dewatering does not occur, there is no separation. Another way of thinking about this mechanism is that the large particles get left behind because of their inertia.

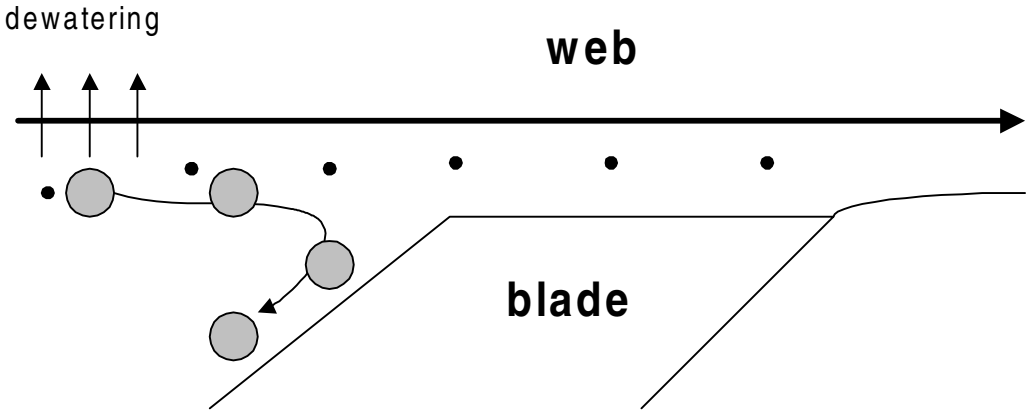


***Figure 8. Proposed mechanism for particle fractionation. Fine particles react to pulse dewatering and move relative to the large particle near the separation streamline.***

***Calculations***

The equations are developed in detail in the Appendix. The basic idea is to calculate the relative motion of particles of different size classes during a dewatering event. The relative motion can then be related to a flux rate of a particle size class. If this flux rate is applied to a mass balance, we can predict the change in concentration.

**Figure 9** illustrates the displacement of particles towards the web, as a function of particle size for a pulse velocity of 1 m/s, a pulse duration of 10 $\mu$s, a particle density of 2500 kg/m3, and a liquid viscosity of 1.0 mPas. These parameters should be in the range of paper coating, except the velocity pulse magnitude may be larger than expected in these situations and is used for illustrative purposes. The fine particles (less than 0.2 microns) move with the fluid phase, but larger particles are left behind. For other conditions, this reduction of motion will occur for different size ranges, but it should always be present.

The key equation in the appendix is Eq. (A7) that shows how rapidly the concentration of a particle in size class "I" will change relative to the bulk fluid. For particles with a significant diameter, this flux rate can be high. An artifact of the analysis is that the large particles can reach flux rates higher than possible based on the current population, and another equation is used to limit the predictions.

A more detailed analysis including the variable flux of the particle size classes as a function of position is possible. We have applied the simplifying assumption that the velocity pulse is turned on and off instantaneously. Our purpose at this point is to see if the proposed mechanism is reasonable and gives the correct order of magnitude results.

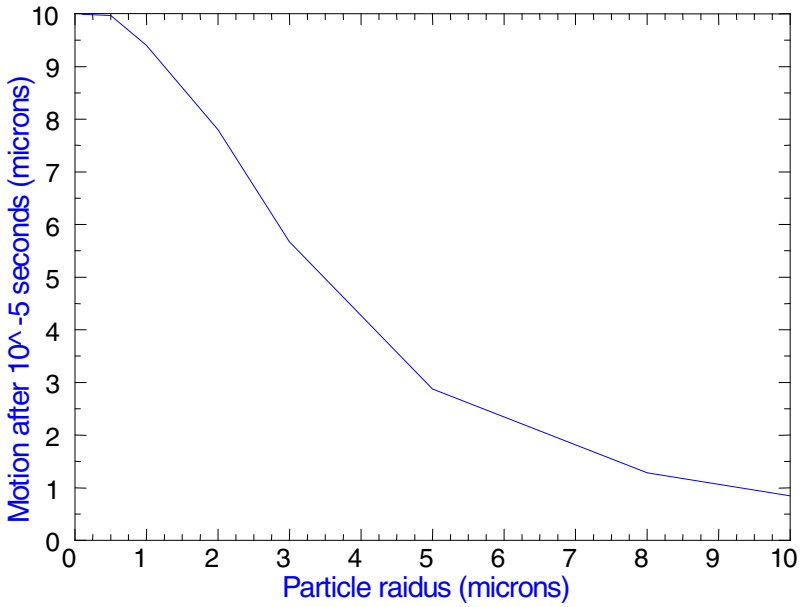


***Figure 9. The displacement of spheres of various radii to an applied velocity pulse. The time to respond is 1 x $10^{-5}$s.***

## *COMPARISON WITH PRODUCTION SCALE DATA*

Returning to Case 1) a comparison of production data regarding particle size distribution may be made to that which is predicted by our proposed mechanism. Several other pieces of information regarding this trial are as follows:

- The coating formula was 50 parts calcium carbonate, 50 parts hydrous kaolin and 18 parts of synthetic binder. This formula was applied to a 5.0 meter (200 inch) trim web using the production unit. The line speed of the machine was 11 m/s (2000 ft/min).

- The target coat weight was 17.5 gm/$m^2$ (12 lb/3300 $ft^2$). A nearly constant dilution flow rate of 5.7 liters/min (1.5 gal/min) was used to control coat weight.

- The recycle rate (gallons of coating supplied to the coater: gallons applied to the web) was approximately 25:1.

- The machine supply tank contained approximately 760 liters (200 gal) of coating. The level of this tank was controlled automatically through the introduction of fresh coating from a bulk supply.

Assuming a pulse dewatering length of 0.1 mm in the machine direction, the average pulse dewatering velocity is estimated to be 0.5 m/s. The pulse time is taken to be 0.01 ms. This would result in about 5 µm of coating dewatered and about 3.5 µm thick filtercake. This magnitude of this pulse velocity may be larger than reality and its duration shorter, but if smaller magnitudes are used, less separation is predicted. Different particle sizes react differently to this pulse. **Figures 10** and **11** show the experimental particles size distribution, obtained with a Sedigraph 5000ET, and the predictions from the model using the particle size diameter in the table. For both cases, we take the liquid viscosity to be 1 mPas, the particle density to be 2500 kg/m3. Eq. (5) and Eq. (7) are used to calculate the change in particle volume fraction over a

given time interval. If the flux rate is greater than the maximum possible, in Eq. (8), then the maximum is used. This maximum was used for the large particle size (5 micron) only. The particle size fractions are obtained by calculating the increase in the volume fraction that is proportional to the weight fraction assuming the particle density is constant. The new volume fractions are normalized after the changes are calculated for each size. The results are encouraging in that the large particles increase in population while the fine particles decrease both experimentally, and predicted by the theory.

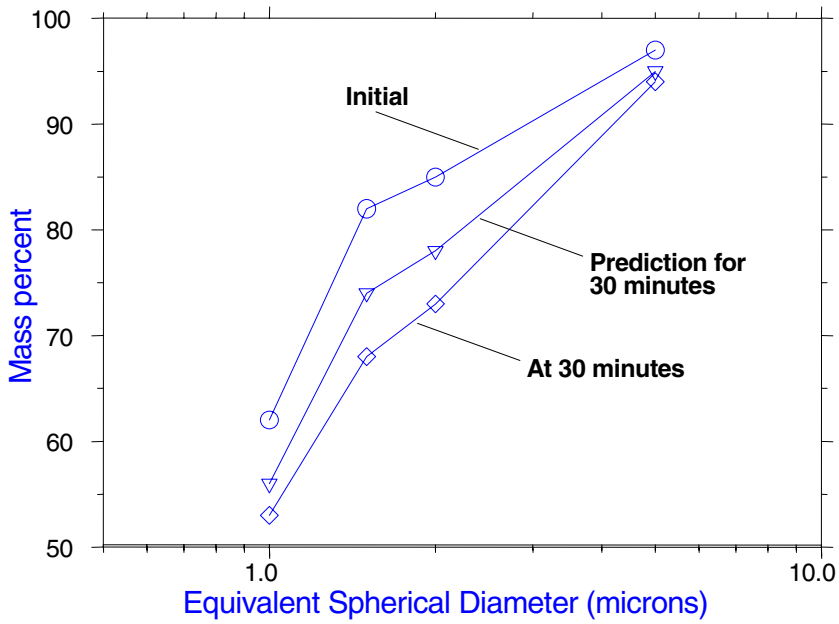


***Figure 10. The measured and predicted particle size distribution for case 1. Model parameters are given in the text.***

For high values of velocity pulse, and typical values for fluid and particle properties, the theory does a reasonable job of predicting the particle size distribution. The very initial stages of dewatering may have this high of velocity pulse because there is little resistance to flow before a filtercake forms on the paper. The large dependence on flux rate with particle size gives the result that large particles easily are left behind by the pulse, while particles less than one micron, move with the fluid phase. The decrease in binder content could be predicted also with the theory, but the results are not reported here. There are a number of assumptions that go into a theory like this, but the general correct trends in the data are well predicted. The colloidal interactions, particle shape, and other issues will change the situation, but this result at least sets the stage for future work.

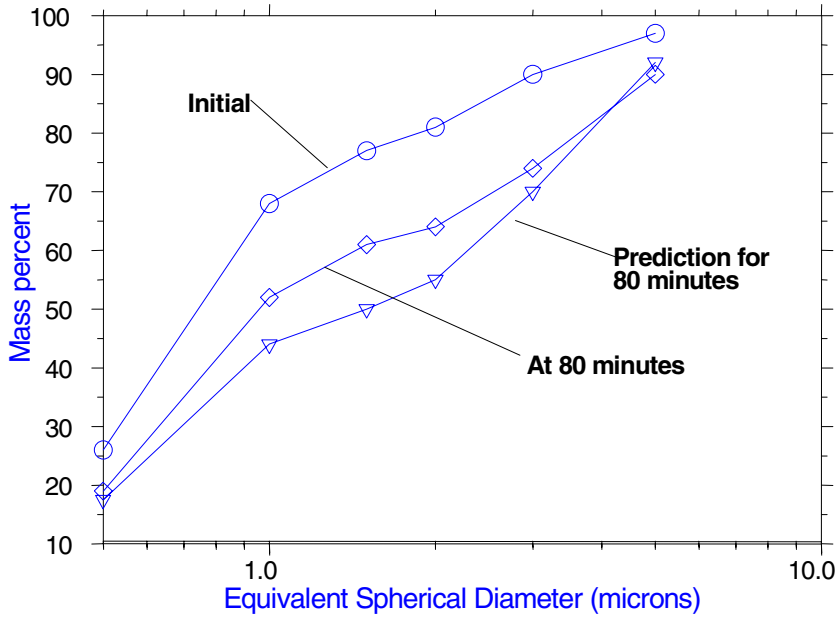


***Figure 11. The measured and predicted particle size distribution for case 2. Model parameters are given in the text.***

## CONCLUSIONS

Coating fractionation is a real-world phenomenon with serious consequences for productivity and quality. The data presented here demonstrate that changes in the pigment particle size distribution of production coatings, (with significant increases in the large particle fraction) and binder depletion impacted sheet properties such as paper gloss and sheet stiffness. The data also showed time dependant changes in the rheologic properties of these same production coatings. The reported decreases in coating viscosity at equal solids are consistent with both and increasingly coarse pigment particle size distribution, and decreasing total organic content. Mill personnel should not neglect the possible involvement of coating fractionation as they seek the sources of time dependant changes in their processes and their products.

The unique mechanism proposed here explains the twin phenomena of particle size segregation and binder (organic) depletion, and is consistent with industrial experience. The theoretical predictions are compared with data from a commercial unit. The proposed mechanism is not proven in this paper, but should be considered as one possible mechanism. Further work to establish the relative effect of basestock properties, coating formula and process (application / metering) parameters on coating fractionation should be conducted. Such work will provide insight into potential approaches to minimize the degree to which coating fractionation can produce downstream effects on productivity and quality.

**ACKNOWLEDGEMENT**

D.W.B. would like to thank the sponsors of the University of Maine Paper Surface Science Program. R.E.G. and T.D.P. would like to acknowledge the contributions of the Technical Service group at Potlatch's Cloquet MN mill, and to thank both Potlatch Corporation and Protein Technologies Int'l for their support in the preparation of this manuscript. Special thanks to; Donald F. Hiscock and Tam H. Tran of Protein Technologies Int'l, Ms Valerie R. Krause of Potlatch Corporation, and Mr. Alan E. Nelson of Michigan Technological University.

**LITERATURE**

1. Bousfield, D. W., "Prediction of Velocity and Coat Weight Limits Based on Filtercake Formation", *TAPPI J,* **77(7):** 161-171 (1994).
2. Brotz, F., H. Hanciogullari, and H. G. Wagner, "Analysis of coating color runnability considering the effect of dewatering Part 2: Numerical simulation of the complete coating process", pp 9-26, 1997 Advanced Coating Fundamentals Symposium, TAPPI Press, Atlanta GA 1997.
3. Chen, K. S. A. and L. E. Scriven, "Liquid Penetration into a Deformable Porous Substrate", TAPPI J., 73(1): 151-161 (1990)
4. Coyle, D. J., "Forward Roll Coating with Deformable Rolls: a simple one-dimensional Elasto-Hydrodynamic model", Chem. Eng. Sci., 43:2673 (1998)
5. Eklund, D. and Kahila, S. J., "Processes Occurring under the Blade during Blade Coring", Wochbl. Papierfabr. 106: 661-665 (1978).
6. Eklund D. E. and Salminen P. "Water Transport in the Blade Coating Process", TAPPI J. 69: 116 (1986):
7. Lennartz, J. W., M. B. Gorensek, and R. J. Adler, "Separation of fine-particle dispersions using periodic flows in a spinning coiled tube part II: Batch fractionation experiments", AIChE J. 33(3): 506-509 (1987).
8. Letzelter P. and D. Eklund (1993): Coating color dewatering in blade coaters, Proc. TAPPI Coating Conf., TAPPI PRESS, Atlanta, pp. 247-257.
9. Lohmander S., Martinez M., Lason L., Rigdahl M. and Li T Q "Dewatering of Coating Dispersion – Model Experiments and Analysis", Tappi Advanced Coating Fundamentals Symposium Proceedings, TAPPI Press, 43 (1999).
10. Wineland, J. D. Adler, R. and M. A. Petrik, Fractionation of fine particle slurries using periodic flows in a spinning helix, AIChE J. 35(5): 856-860 (1989).
11. Salminen P. J., Roper J., Pollock M., and Chonde Y., "Determining the Dynamic Water Retention Contribution of Various Cobinders and Thickeners", TAPPI Coating Conference Proceedings, TAPPI Press, pp. 277-284 (1995)
12. Toivakka, M. and D. Eklund, "Prediction of suspension rheology through particle motion simulation", TAPPI J. 79:211-222 (1996).

Received: November 10, 2000
Accepted: November 10, 2000

This paper was accepted for abstracting and publication in the May 2001 issue of *TAPPI JOURNAL.*

*TAPPI Website: www.tappi.org*

## APPENDIX

The viscous drag on a sphere relative to a velocity of $v_p$ is given by

$$F = 6\pi\mu a(v_p - v) \tag{A1}$$

Where $\mu$ is the viscosity, $a$ is the sphere radius, and $v$ is the velocity of the sphere. The mass of the sphere is given by the sphere density multiplied by its volume.

$$m = \frac{4\pi a^3 \rho_p}{3}; \tag{A2}$$

Where $\rho_p$ is the density of the particle.

Using Newton's law of motion, $F=må$, we can calculate the acceleration of the sphere to an applied velocity pulse.

If the initial velocity of the sphere is zero, relative to the web, then the velocity of the sphere, at any time, can be calculated by integrating the acceleration term. The result is

$$v = v_p\left(1 - \exp\left(\frac{-9\mu t}{2a^2\rho_p}\right)\right) \tag{A3}$$

As time gets large, the particle reaches the velocity of the fluid pulse. This exponential response is expected from this type of problem. Small particles are quick to respond to the fluid forces because of their small mass. They do have a smaller force, as Eq. (1) applied to them, but their mass scales to the third power of the radius.

The displacement of the particle, as a function of time, comes from integrating the velocity equation. The results is

$$\Delta x = v_p\left(t + \frac{2a^2\rho_p}{9\mu}\exp\left(\frac{-9\mu t}{2a^2\rho_p}\right)\right) - \frac{2v_p a^2\rho_p}{9\mu} \tag{A4}$$

Now, given a velocity pulse, and its time duration, we can predict the motion of a particle toward the web.

If we use half the pulse time to calculate the velocity of the particles, we get an idea of the mass flux of the particles towards the web. The difference between this velocity and the fluid phase velocity can be thought of a flux of particles away from the web and back toward the recycle loop. This flux rate, for a particle of radius $a_i$ is

$$N_i = v_p\left(\exp\left(\frac{-9\mu t_p}{4a_i^2\rho_p}\right)\right) \tag{A5}$$

Where $N_i$ is the flux rate of particles of size, i away from the web and $t_p$ is the time duration of the pulse dewatering. Notice that the flux rate is a strong function of the particle radius. The picture would be different in a crowded concentration, but this is a reasonable start. A mass balance around the nip exit completes the picture. The increase in the concentration of particle size i, as a function of time is given by;

$$\frac{dV\phi_i}{dt} = N_i A - Q_d \tag{A6}$$

where $\phi$ is the volume fraction of size category i, V is the volume of coating in the supply tank, and A is the area available for particle fractionation. This area is equal to the trim width of the machine multiplied by the pulse duration. If the volume of coating in the supply tank is approximately constant, then the increase in the particle concentration is calculated as

$$\frac{d\phi_i}{dt} = N_i A / V - Q_d / V \tag{A7}$$

The flux rate in Eq. (5) assumes an unlimited source of particles in the region of separation. The equation would predict a large flux rate for large particles, regardless of the population of large particles. Therefore, straight application of the equation could lead to unrealistic predictions. The flow rate of particles along a region of the stagnation streamline is a limiting source of particles of each size range. The maximum flux rate, therefore, would be the flux rate of large particles coming into the separation region and can be given as

$$N_{i,\max} = U\phi_i \frac{h_s}{L_p} \tag{A8}$$

where U is the web velocity, $h_s$ is the height of the separation zone, and $L_p$ is the length of the pulse duration. Often, dilution water is added (more or less) continuously to the supply tank to control coating solids and therefore any one of a number of process parameters. This dilution water flow rate should match the increase in solids during the coating operation. Notice that every particle size category will have its own "flux" rate, with small particles having small flux rates and large particles having large flux rates, up to the value of the velocity pulse.